Endocrinology. First published ahead of print January 17, 2012 as doi:10.1210/en.2011-1954

Disruption of the Murine *Glp2r* Impairs Paneth Cell Function and Increases Susceptibility to Small Bowel Enteritis

Seung-Jun Lee, Jennifer Lee, Karen K. Li, Dianne Holland, Heather Maughan, David S. Guttman, Bernardo Yusta, and Daniel J. Drucker

Department of Medicine, Mt. Sinai Hospital, Samuel Lunenfeld Research Institute (S.-J.L., J.L., K.K.L., D.H., B.Y., D.J.D.), and the Department of Cell and Systems Biology (H.M., D.S.G.), University of Toronto, Toronto Ontario, Canada M5G 1X5

Exogenous glucagon-like peptide-2 receptor (GLP-2R) activation elicits proliferative and cytoprotective responses in the gastrointestinal mucosa and ameliorates experimental small and large bowel gut injury. Nevertheless, the essential physiological role(s) of the endogenous GLP-2R remain poorly understood. We studied the importance of the GLP-2R for gut growth, epithelial cell lineage allocation, the response to mucosal injury, and host-bacterial interactions in *Glp2r*$^{-/-}$ and littermate control *Glp2r*$^{+/+}$ mice. *Glp2r*$^{-/-}$ mice exhibit normal somatic growth and preserved small and large bowel responses to IGF-I and keratinocyte growth factor. However, *Glp2r*$^{-/-}$ mice failed to up-regulate intestinal epithelial c-fos expression in response to acute GLP-2 administration and do not exhibit changes in small bowel conductance or small or large bowel growth after administration of GLP-2R agonists. The crypt and villus compartment and the numbers and localization of Paneth, enteroendocrine, and goblet cells were comparable in *Glp2r*$^{+/+}$ vs. *Glp2r*$^{-/-}$ mice. Although the severity and extent of colonic mucosal injury in response to 3% oral dextran sulfate was similar across *Glp2r* genotypes, *Glp2r*$^{-/-}$ mice exhibited significantly increased morbidity and mortality and increased bacterial translocation after induction of enteritis with indomethacin and enhanced mucosal injury in response to irinotecan. Moreover, bacterial colonization of the small bowel was significantly increased, expression of Paneth cell antimicrobial gene products was reduced, and mucosal bactericidal activity was impaired in *Glp2r*$^{-/-}$ mice. Although the *Glp2r* is dispensable for gut development and the response to colonic injury, *Glp2r*$^{-/-}$ mice exhibit enhanced sensitivity to small bowel injury, and abnormal host-bacterial interactions in the small bowel. **(*Endocrinology* 153: 0000–0000, 2012)**

Glucagon-like peptide-2 (GLP-2) is a member of the proglucagon-derived peptide family produced in gut endocrine L cells. GLP-2 is secreted at low basal levels in the fasting state and its circulating levels rise rapidly after nutrient ingestion (1). Exogenous administration of GLP-2 expands the small and large bowel mucosa through stimulation of crypt cell proliferation and inhibition of cell death (2). These actions of GLP-2 are conserved in the setting of experimental intestinal injury, leading to preservation and/or regeneration of damaged mucosal epithelium.

GLP-2 also increases intestinal blood flow (3, 4) and gut barrier function (5) and enhances nutrient absorption via stimulation of glucose transport activity (6, 7). Moreover, GLP-2 infusion enhances lipid absorption and chylomicron secretion in mice (8) and increases postprandial levels of triglycerides and free fatty acids in normal human subjects (9). The ability of GLP-2 to enhance nutrient absorption has led to its evaluation for the treatment of short bowel syndrome. Once- or twice-daily administration of a GLP-2 analog, teduglutide, increased the nutrient absorption and reduced energy

ISSN Print 0013-7227 ISSN Online 1945-7170
Printed in U.S.A.

doi: 10.1210/en.2011-1954 Received November 5, 2011. Accepted December 20, 2011.

Abbreviations: BrdU, 5-Bromo-2′-deoxyuridine; DS, dextran sulfate; ErbB, erythroblastic leukemia viral oncogene homolog; GLP-2, glucagon-like peptide-2; GLP-2R, GLP-2 receptor; KGF, keratinocyte growth factor; LPS, lipopolysaccharide; rHu, recombinant human.

malabsorption in human subjects with short bowel syndrome (10, 11).

Despite the delineation of multiple actions arising after exogenous pharmacological GLP-2 administration, the endogenous physiological action(s) of GLP-2 remain less well defined. Acute administration of a GLP-2 antagonist GLP-2 (3–33) partially attenuates the normal adaptive response of the small bowel mucosa to fasting/refeeding through modulation of crypt cell proliferation and apoptosis (12, 13). Similarly, attenuation of circulating GLP-2 bioactivity using immunoneutralizing antibodies reduced the extent of adaptive mucosal hyperplasia in rats with streptozotocin-induced diabetes (14).

Elucidation of mechanisms underlying endogenous GLP-2 action has been challenging in part due to the limitations of available GLP-2 receptor antagonists and the complexity of the cellular localization of GLP-2 receptor signaling. The antagonist GLP-2 (3–33) is also a weak partial agonist (12, 15), limiting its suitability for complete sustained blockade of GLP-2 action *in vivo*. Moreover, transient selective reduction of GLP-2 receptor (GLP-2R) expression is challenging because the GLP-2R is expressed on rare subsets of enteric neurons, enteroendocrine cells, and myofibroblasts and exerts its actions indirectly, through activation of incompletely characterized downstream mediators (16–18).

To delineate the importance of the endogenous GLP-2R, we generated mice with targeted inactivation of the gene encoding the GLP-2R. $Glp2r^{-/-}$ mice fail to up-regulate intestinal growth factor expression in response to acute GLP-2 administration (18), manifest defective up-regulation of crypt cell proliferation in response to fasting-refeeding (19), but do not exhibit defects in the intestinal adaptive response to experimental streptozotocin-induced diabetes (20). We now report that germline loss of the *Glp2r* does not result in defects in cell lineage allocation within the gut epithelium, susceptibility to colonic injury, or defective control of intestinal permeability. However $Glp2r^{-/-}$ mice demonstrate increased susceptibility to mucosal injury induced by indomethacin or irinotecan in the small bowel. Furthermore, $Glp2r^{-/-}$ mice exhibit defective Paneth cell function as evidenced by reduced expression of defensins and impaired bactericidal activity *ex vivo*. Moreover, the small bowel of uninjured $Glp2r^{-/-}$ mice exhibit significantly increased numbers of bacteria, and microbiome analysis demonstrates a significant shift in the proportion of *Firmicutes*, *Bacteroidetes*, and *Actinobacteria* phyla in the feces. These findings reveal that basal GLP-2R activity is essential for the prevention of mucosal injury in the small bowel and the maintenance of normal host-bacteria interactions along the gastrointestinal tract.

Materials and Methods

Animals

$Glp2r^{-/-}$ mice were generated in the C57BL/6 background by replacing exons 7–9 of the *Glp2r* with a neomycin resistance cassette inserted in the opposite direction to that of *Glp2r* transcription (Supplemental Fig. 1, published on The Endocrine Society's Journals Online web site at http://endo.endojournals.org). The genotyping strategy is shown in Supplemental Fig. 2. The wild-type $Glp2r^{+/+}$ littermates were used as controls for all studies involving $Glp2r^{-/-}$ mice. Studies were performed on either male or female mice, as indicated in the figure legends, aged 8–12 wk, that were bred at the Toronto Centre for Phenogenomics Animal facility. All animal experiments were approved by the Animal Care Committee of the Mount Sinai Hospital.

Peptide and drug treatments

Human [Gly^2]GLP-2, hence referred to as GLP-2, was from Pepceutical Ltd. (Nottingham, UK), Long-R^3-IGF-I (recombinant human IGF-I) was from Gropep Ltd. (Adelaide, Australia) and recombinant human (rHu) keratinocyte growth factor (KGF) was obtained from Amgen Inc. (Thousand Oaks, CA). GLP-2 and Long-R^3-IGF-I were administered sc, whereas rHuKGF was injected into the peritoneum (ip). All peptides were administered in PBS. Experiments involving analysis of dextran sulfate colitis and indomethacin- or irinotecan-induced enteritis were carried out as previously described (21–23). To assess intestinal crypt cell proliferation 5-bromo-2′-deoxyuridine (BrdU; Sigma-Aldrich, Oakville, Ontario, Canada; 100 mg/kg) dissolved in PBS was injected ip to mice 1 h before the animals were killed.

Tissue collection and processing for morphometry and immunohistochemistry

Intestinal tissue was collected, flushed with PBS, fixed in 10% neutral buffered formalin, and paraffin embedded. Histomorphometry was performed on 5-μm sections stained with hematoxylin and eosin, using a Leica Q500MC Image Analysis System (Leica Inc., Cambridge, UK). Villus height and crypt depth were measured on 12 cross-sections with an average of 20 measurements per mouse. Immunohistochemistry was carried out using indirect immunoperoxidase detection with NovaRED substrate (Vector Laboratories, Burlington, Ontario, Canada) followed by hematoxylin counterstaining. Antilysozyme and antisynaptophysin rabbit polyclonal antibodies (DakoCytomation, Mississauga, Ontario, Canada) were used to quantify Paneth and enteroendocrine cell populations, respectively. BrdU incorporation was detected using a mouse monoclonal anti-BrdU antibody (Invitrogen Canada, Burlington, Ontario, Canada) and c-fos protein using a rabbit polyclonal anti-c-fos antibody (Sigma-Aldrich). Periodic acid-Schiff staining was used to visualize goblet cells.

Intestinal permeability

Two to three contiguous segments of proximal and midjejunum were cut along the mesenteric border, mounted in modified Ussing chambers (EasyMount chambers; Physiologic Instruments, San Diego, CA), and bathed with Kreb's buffer [140 mM NaCl, 1.2 mM $CaCl_2$, 1.2 mM $MgCl_2$, 10 mM $KHCO_3$, 0.2 mM KH_2PO_4, and 1.2 mM K_2HPO_4 (pH 7.4)] at 37 C with contin-

uous oxygenation. Glucose (10 mM) was added to the buffer at the serosal surface balanced by 10 mM mannitol in the buffer at the mucosal surface. After equilibration for 20 min, tissues were short circuited at zero volts using an automatic multichannel voltage/current clamp (model VCC MC8; Physiologic Instruments). Tissue conductance was calculated according to Ohm's law using potential difference and short circuit current values. Average short circuit current and conductance values were determined using Acquire and Analyze software (Physiologic Instruments).

Western blot analysis

Whole-tissue extracts were prepared by homogenization of intestinal segments in radioimmunoprecipitation assay buffer (1% Nonidet P-40, 0.5% sodium deoxycholate, and 0.1% sodium dodecyl sulfate in PBS) supplemented with protease and phosphatase inhibitors (Sigma-Aldrich), 5 mM sodium fluoride, and 200 μM sodium orthovanadate. Lectin adsorption was carried out using wheat germ agglutinin-agarose (EMD Chemicals Inc., Gibbstown, NJ) and elution with 0.3 M *N*-acetyl-D-glucosamine, as previously reported (24). Western blot analysis of lectin pull-down proteins was performed as described (25). GLP-2R antisera were generously provided by Professor Jens Holst (University of Copenhagen, Copenhagen, Denmark) (16).

Microbiology

Whole blood was obtained by cardiac puncture. Spleen, liver, and mesenteric lymph nodes were removed and homogenized in sterile PBS. Aliquots of whole blood and tissue homogenates were plated on blood agar plates and incubated at 37 C for 24–48 h under aerobic conditions before assessing the presence of bacterial colonies or quantifying the percent of the blood agar plate surface that underwent hemolysis. To determine small intestinal aerobic bacterial load, the luminal contents were collected by flushing with PBS. The number of colony-forming units per mouse small intestine was determined by plating serial dilutions of the flushed material on blood agar plates and counting colonies after incubation at 37 C for 24 h.

RNA isolation and quantitative real-time RT-PCR

Total RNA from intestinal tissue was extracted by the guanidinium thiocyanate method and cDNA synthesis performed with random hexamers and SuperScript II (Invitrogen). Real-time quantitative PCR was performed on an ABI PRISM 7900HT sequence detection system (Applied Biosystems, Foster City, CA) with TaqMan universal PCR master mix and TaqMan gene expression assays (Applied Biosystems) for *glp2r* (Mm01329473_m1 for exons 2–3 and Mm01329477_m1 for exons 7–8), *lysozyme P* (Mm00657323_m1), *defcr-rs1* (Mm00655850_m1), *cryptdin 5* (Mm00651548_g1), *pla2g2a* (Mm00448160_m1), *mmp7* (Mm00487724_m1), *lgr5* (Mm00438890), *epgn* (Mm00504344_m1), *egf* (Mm00438696), *erbB1* (Mm00433023), *igf-1R* (Mm00802831), *il-6* (Mm00446190), *myd88* (Mm00440338), *nfkb* (Mm00476361), *mip-2* (Mm00436450), *il-33* (Mm00505403), *cxcl-10* (Mm00445235), and *il-15* (Mm00434210). Relative quantification of transcript levels was performed by the $2^{-\Delta\Delta Ct}$ method using the cycle threshold values obtained from the PCR amplification kinetics with the ABI PRISM SDS 2.1 software. 18S rRNA or cyclophilin was used for normalization because its intestinal expression remained unaltered, regardless of mouse genotype or treatment.

Crypt isolation, stimulation of Paneth cell secretion, and bactericidal activity assays

Small intestinal crypts were isolated after incubation of the tissue at room temperature in Ca^{2+}- and Mg^{2+}-free PBS containing 30 mM EDTA (26). Paneth cell secretion from the isolated crypts was induced by stimulation with the cholinergic agonist carbamylcholine (10 μM; Sigma-Aldrich) or the Toll-like receptor 4 agonist lipopolysaccharide (LPS; purified from *Escherichia coli* 0111:B4, 10 μg/ml; Sigma-Aldrich) for 30 min at 37 C. Crypt secretions were recovered by centrifugation and their bactericidal activity assayed against 5×10^6 colony-forming units *E. coli* DH5α as described (27).

Microbial genomic DNA extraction and analysis of the 16S rRNA locus

Fresh cecum and fecal pellets were collected and immediately frozen at −80 C. Samples were ground in liquid nitrogen and DNA extracted after microbial cell lysis with zirconia/silica beads as described (28). DNA fragments were sequenced by amplifying the 16S rRNA locus from each DNA sample using barcoded primers. Amplicons were pooled and carried through the standard Illumina paired-end sample prep. Six sequence reads were obtained (three from each strand); one sequence read from each strand corresponded to the sample-specific barcode (8 bp). The remaining four sequence reads (36 bp each) corresponded to the V5, V6, and V7 hypervariable regions of the 16S rRNA locus. These reads were concatenated and assigned bacterial taxonomies using the Ribosomal Database Project classifier (29), which had been trained using the Bergey database of sequences modified to have the same 36- × 4-bp read structure (rather than full length 16S rRNA sequences).

Statistics

Results are expressed as mean ± SE. Comparisons between genotype and/or treatment groups were performed by one- or two-way ANOVA followed by the Bonferroni or Fisher *post hoc* test. The χ^2 test was used to analyze the data (see Fig. 3, A and C). Comparison between Kaplan-Meier survival curves shown (see Fig. 3B) was performed using the log-rank test. Statistical analyses were carried out using the GraphPad Prism 4 software package (GraphPad Software Inc., San Diego, CA) and Statistica 6 (StatSoft Inc., Tulsa, OK).

Results

Glp2r$^{-/-}$ mice were born at expected Mendelian frequencies and appeared healthy, and both body weight (Fig. 1A) and food intake (Supplemental Fig. 3) were comparable in *Glp2r*$^{+/+}$ *vs.* *Glp2r*$^{-/-}$ mice. *Glp2r* mRNA transcripts corresponding to the targeted exons and immunoreactive GLP-2R protein were detected in intestinal tissues from *Glp2r*$^{+/+}$ and *Glp2r*$^{+/-}$ but not *Glp2r*$^{-/-}$ mice (Supplemental Fig. 4, A and B). A single 5-μg injection of h[Gly^2]-GLP-2 significantly increased nuclear c-fos expression in

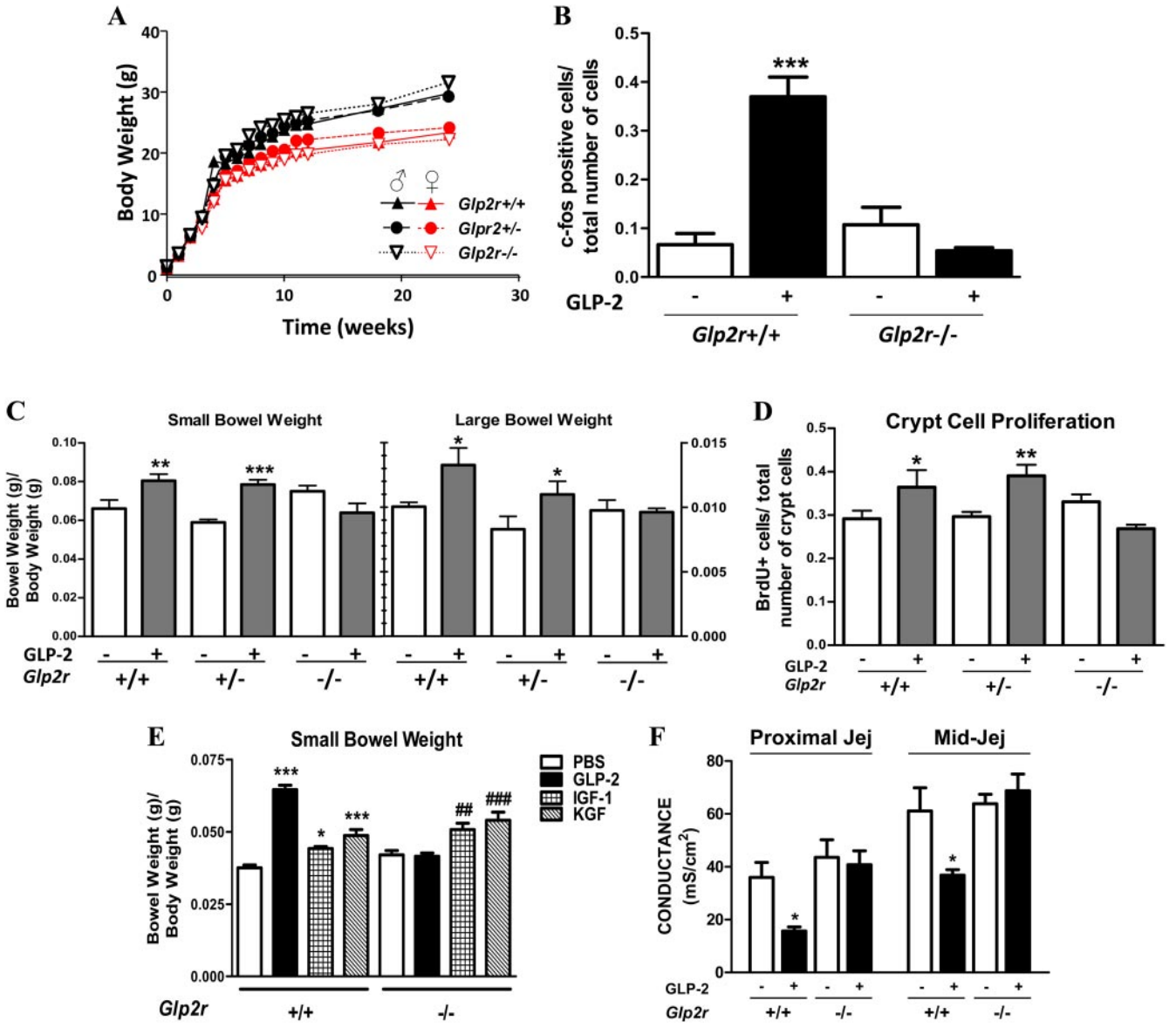

FIG. 1. Characterization of *Glp2r*$^{-/-}$ mice. A, Body weights of male and female *Glp2r*$^{+/+}$, *Glp2r*$^{+/-}$, and *Glp2r*$^{-/-}$littermates (n = 4 per group) over 24 wk. B, The c-fos-immunopositive cell number in the jejunal epithelium of *Glp2r*$^{+/+}$ and *Glp2r*$^{-/-}$ male mice (n = 3–4 per group) 1 h after GLP-2 (5 μg) administration. Small and large bowel weights (C) and jejunal crypt cell proliferation (D) after the administration of saline or GLP-2 (10 μg once daily) for 7 d in female *Glp2r*$^{+/+}$, *Glp2r*$^{+/-}$, and *Glp2r*$^{-/-}$ littermates (n = 7–8 per group). E, Small bowel weight in response to GLP-2 (2.5 μg twice daily), Long-R^3-IGF-I (25 μg twice daily), or rHuKGF (5 mg/kg body weight once daily) administration to female *Glp2r*$^{+/+}$ and *Glp2r*$^{-/-}$ mice for 10 d (n = 5–6 per group). F, The jejunal (Jej) transmural ion conductance from female *Glp2r*$^{+/+}$ and *Glp2r*$^{-/-}$ mice (n = 3–6 per group) administered saline or GLP-2 (5 μg twice daily) for 9 d. *, $P < 0.05$, ** or ##, $P < 0.01$, *** or ###, $P < 0.001$, treatment *vs.* vehicle control.

the epithelium of the jejunum (Fig. 1B and Supplemental Fig. 5) and colon (Supplemental Fig. 6) of *Glp2r*$^{+/+}$ but not in *Glp2r*$^{-/-}$ mice. Basal levels of small and large bowel weight (Fig. 1C), jejunal villus height and crypt depth, colon crypt depth (Supplemental Figure 7), crypt cell proliferation, and jejunal conductance (Fig. 1, D and F) were comparable in *Glp2r*$^{+/+}$ *vs.* *Glp2r*$^{-/-}$ mice. Sustained h[Gly^2]-GLP-2 administration produced a robust intestinotrophic response in the small and large bowel of *Glp2r*$^{+/+}$ mice but had no effect on jejunal ion conductance, small or large bowel weight, small bowel villus height, crypt depth, colonic mucosal thickness, DNA content, small bowel ion conductance, or crypt cell proliferation in *Glp2r*$^{-/-}$ mice (Fig. 1, C–F, and Supplemental Fig. 7). In contrast, administration of IGF-I or KGF increased small bowel mass (Fig. 1E) and KGF increased colonic mass (Supplemental Fig. 8) in *Glp2r*$^{+/+}$ and *Glp2r*$^{-/-}$ mice. Cell lineage allocation (Goblet, enteroendocrine, and Paneth cells) was also comparable in *Glp2r*$^{+/+}$ *vs.* *Glp2r*$^{-/-}$ mice (Supplemental Figs. 9 and 10). Taken to-

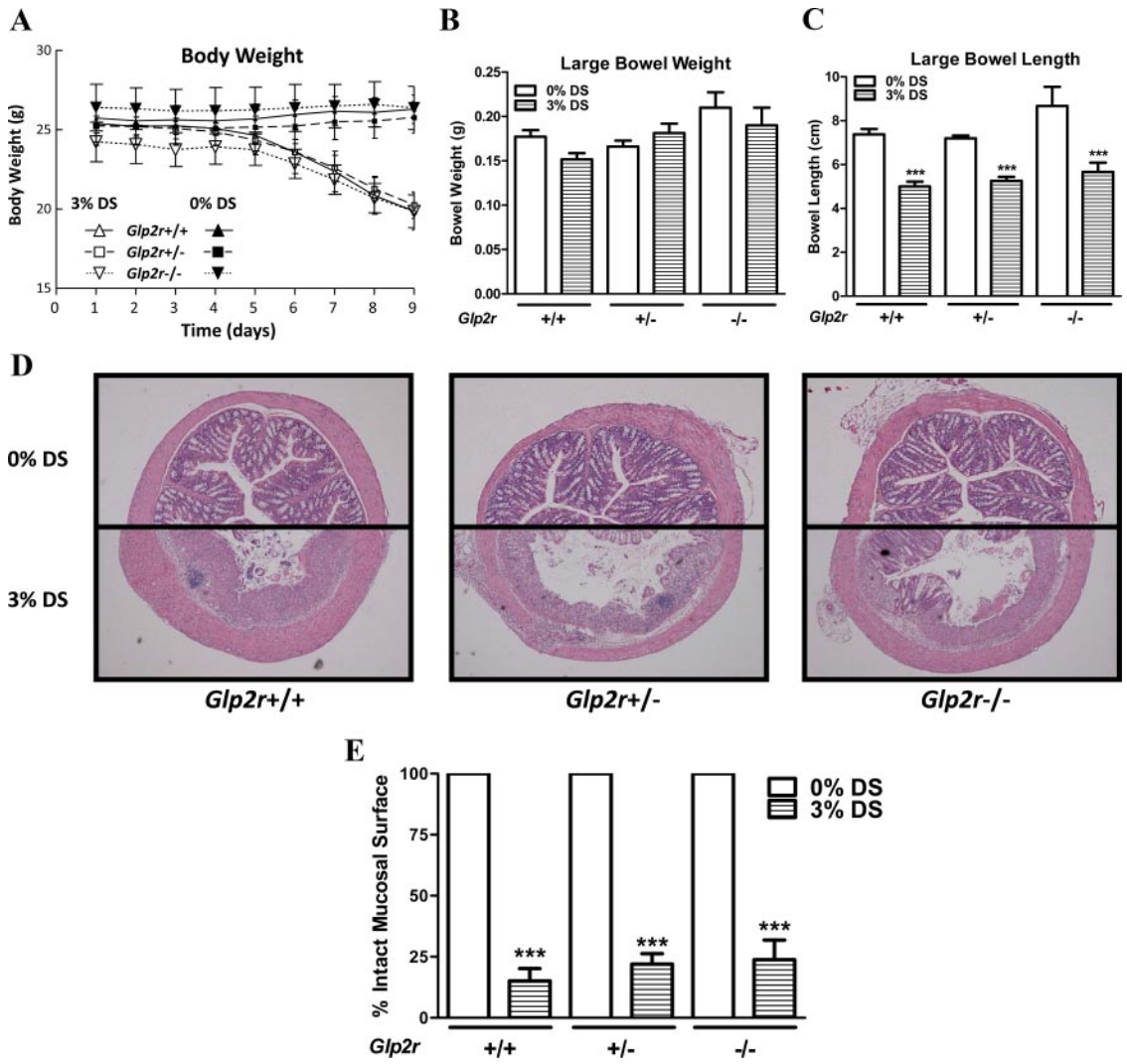

FIG. 2. Body weight (A), large bowel weight (B) and length (C), histology (D), and percentage intact mucosa (E) from male $Glp2r^{+/+}$, $Glp2r^{+/-}$, and $Glp2r^{-/-}$ mice treated with water alone (0% DS) or oral dextran sulfate (3% DS) in the drinking water for 9 d (n = 4–8 per group). ***, $P < 0.001$ 0% *vs.* 3% DS-treated mice. Similar results were obtained in studies of female mice of the same genotypes (data not shown).

gether, these analyses demonstrate that the $Glp2r^{-/-}$ mouse fails to respond to acute or chronic GLP-2 treatment yet exhibits normal epithelial structure and cell composition in the gastrointestinal tract.

Because germline loss of the *Glp2r* was not associated with a demonstrable intestinal phenotype in nonstressed mice, we subjected $Glp2r^{+/+}$, $Glp2r^{+/-}$, and $Glp2r^{-/-}$ mice to experimental dextran sulfate (DS)-induced colitis, a controlled inflammatory insult responsive to exogenous GLP-2 administration (22, 30). Oral administration of 3% DS for 9 d produced comparable weight loss and similar changes in colon weight and length in $Glp2r^{+/+}$ *vs.* $Glp2r^{+/-}$ and $Glp2r^{-/-}$ mice (Fig. 2, A–C). Furthermore, the extent of colonic mucosal injury was similar across *Glp2r* genotypes (Fig. 2, D and E). Body weight gain after recovery from 3% DS for 5–8 d was also unaffected by *Glp2r* genotype (data not shown). Hence, loss of the *Glp2r* does not influence the severity of or recovery from DS-induced colonic injury.

Because *Glp2r* mRNA transcripts are also present in the small bowel (31, 32), we assessed the consequences of nonsteroidal antiinflammatory drug-induced small bowel enteritis in $Glp2r^{-/-}$ mice (21). The proportion of moribund $Glp2r^{-/-}$ mice was significantly higher compared with $Glp2r^{+/+}$ littermate controls 24 h after indomethacin administration (Fig. 3A), and more $Glp2r^{-/-}$ mice succumbed after indomethacin administration (Fig. 3B). We next assessed whether enhanced bacterial infection might underlie the increased morbidity of $Glp2r^{-/-}$ mice. The proportion of indomethacin-treated $Glp2r^{-/-}$ mice exhibiting positive bacterial cultures in liver, spleen, and blood trended significantly higher ($P < 0.01$, χ^2 test for trend) relative to levels in $Glp2r^{+/+}$ mice, and significantly more $Glp2r^{-/-}$ mice exhibited positive mesenteric lymph node bacterial cultures (Fig. 3C).

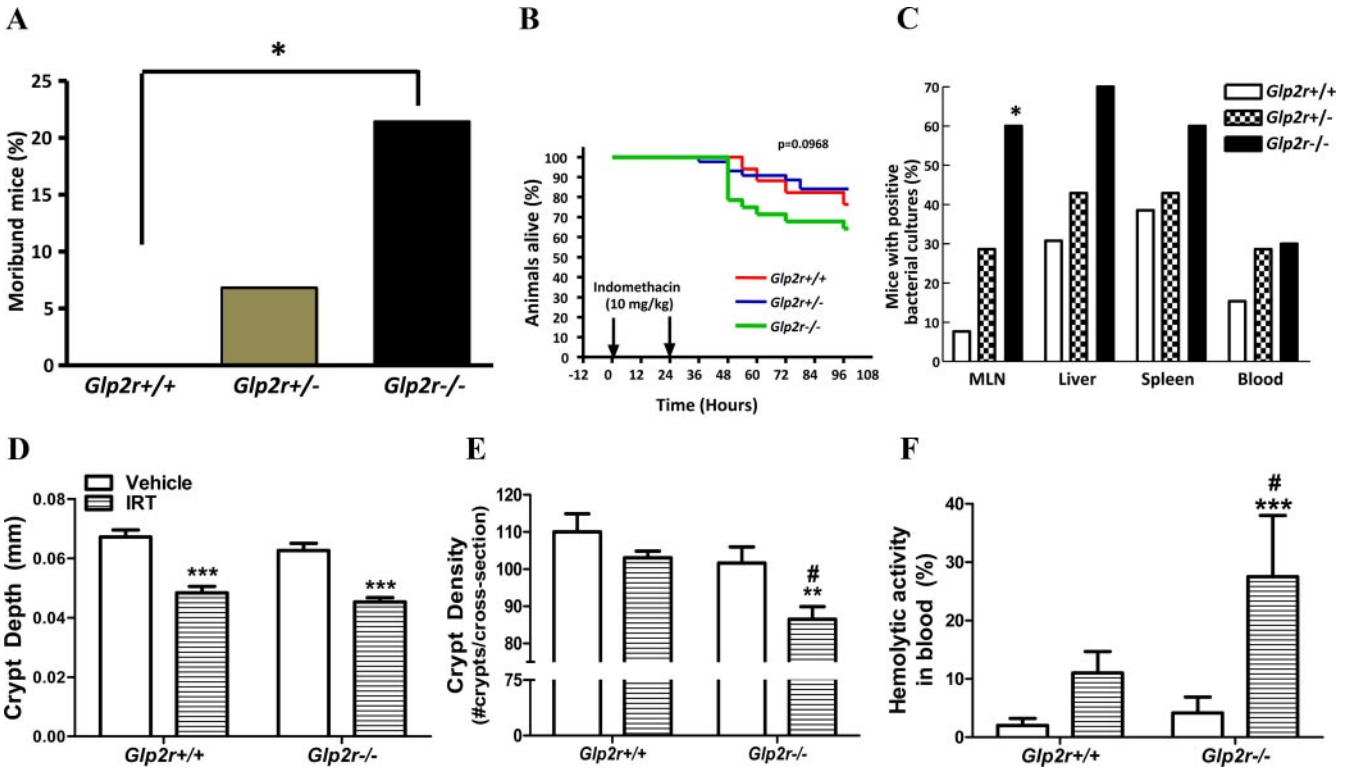

FIG. 3. Indomethacin and irinotecan produce increased small bowel injury in $Glp2r^{-/-}$ mice. Proportion of moribund (A), percent survival (B), and percent positive (C) bacterial cultures in male $Glp2r^{+/+}$, $Glp2r^{+/-}$, and $Glp2r^{-/-}$ mice (n = 17–28 per group) after two sc injections of vehicle or indomethacin. *, $P < 0.05$, $Glp2r^{-/-}$ *vs.* $Glp2r^{+/+}$ (for A and C). Jejunal crypt depth (D) and crypt density (E) and prevalence of hemolytic activity in blood (F), a reflection of bacterial septicemia, in male $Glp2r^{-/-}$ *vs.* $Glp2r^{+/+}$ mice (n = 5–6 per group) 24 h after two ip injections of vehicle or irinotecan (IRT). **, $P < 0.01$, ***, $P < 0.001$ IRT *vs.* vehicle; #, $P < 0.05$, $Glp2r^{-/-}$ *vs.* $Glp2r^{+/+}$.

To determine whether $Glp2r^{-/-}$ mice exhibited enhanced sensitivity to small bowel mucosal injury in a second independent experimental model, we assessed the acute effects of irinotecan, a chemotherapeutic agent with significant gastrointestinal toxicity (23). After irinotecan treatment, jejunal crypt depth was similarly decreased in both $Glp2r^{+/+}$ and $Glp2r^{-/-}$ mice; however, only $Glp2r^{-/-}$ mice exhibited a significant reduction in crypt density (Fig. 3, D and E). Furthermore, hemolysis on blood agar plates, an indirect measure of systemic bacteremia, was increased to a significantly greater extent in $Glp2r^{-/-}$ *vs.* $Glp2r^{+/+}$ mice after irinotecan (Fig. 3F). To explore the basis for the enhanced mucosal damage in response to irinotecan, we assessed expression of genes important for small bowel growth, survival, and inflammation. Irinotecan-treated $Glp2r^{-/-}$ mice exhibited significantly reduced levels of mRNA transcripts for the stem cell marker *lgr5*, the erythroblastic leukemia viral oncogene homolog (ErbB) ligand *EGF*, and the *Igf1r*. Conversely, levels of mRNA transcripts for *epgn* and *ErbB1* were not as up-regulated in irinotecan-treated $Glp2r^{-/-}$ *vs.* $Glp2r^{+/+}$ mice, whereas levels of the mRNA for the cytokine *Il-6* were significantly up-regulated in $Glp2r^{-/-}$ compared with $Glp2r^{+/+}$ small bowel (Fig. 4).

Because increased bacterial infection may reflect altered gut barrier function and microbial colonization, we assessed intestinal bacterial colonization in $Glp2r^{-/-}$ mice. $Glp2r^{-/-}$ mice exhibited a significantly greater bacterial load in the small bowel relative to age and sex-matched littermate controls (Fig. 5A). To identify mechanisms underlying increased small bowel bacterial colonization in $Glp2r^{-/-}$ mice, we determined the expression of Paneth cell genes known to be important for host-bacterial interactions. Although levels of *lysozyme* and the defensin-related *Defcr-rs1 (crypt1)* mRNA transcripts were comparable in the jejunum and ileum of $Glp2r^{-/-}$ *vs.* $Glp2r^{+/+}$ mice, levels of ileal matrix metalloproteinase 7 (*Mmp7*) mRNA, the key enzyme responsible for activation of defensin activity, and the abundance of *cryptdin 5* and secretory phospholipase A2 (*Pla2g2a*) mRNA transcripts were lower in both jejunum and ileum of $Glp2r^{-/-}$ mice (Fig. 5B). Furthermore, we detected significantly reduced intestinal expression of multiple RNA transcripts encoding proteins involved in the host response to infection in $Glp2r^{-/-}$ mice, including *myd88*, *nfkb*, *mip2*, *il-6*, *il-33*, *cxcl10*, and *il-15* (Fig. 5C).

The increased bacterial load, enhanced bacterial translocation, and altered Paneth gene expression signature

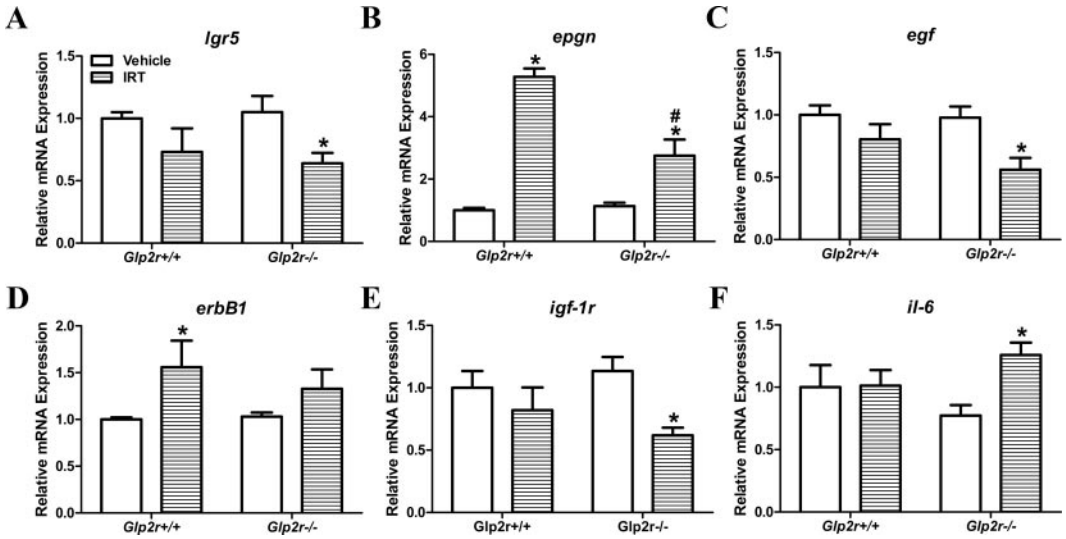

FIG. 4. Defective gene expression in response to irinotecan (IRT) in the small bowel of $Glp2r^{-/-}$ mice. Relative jejunal mRNA levels of *lgr5* (leucine rich repeat-containing G protein coupled receptor 5) (A), *epgn* (epigen) (B), *egf* (epidermal growth factor) (C), *erbB1* (epidermal growth factor receptor) (D), *igf-1r* (IGF-I receptor), (E) and *il-6* (IL-6) (F) from $Glp2r^{+/+}$ and $Glp2r^{-/-}$ male mice (n = 4–6 per group) treated with IRT. *, $P < 0.05$, IRT *vs.* vehicle; #, $P < 0.05$, $Glp2r^{-/-}$ *vs.* $Glp2r^{+/+}$.

suggested the presence of a functional Paneth cell defect. Consistent with this hypothesis, Paneth cell secretions isolated from $Glp2r^{-/-}$ mice exhibited reduced bactericidal activity after stimulation with carbamylcholine and LPS *ex vivo* (Fig. 5D).

To further explore whether loss of the *Glp2r* impaired host-microbiome interactions, we assessed the proportion of key bacterial phyla in the cecum and feces of $Glp2r^{-/-}$ mice. A number of significant differences were detected in the representation of specific fecal bacterial populations, including significant reductions in the proportions of *Firmicutes* and *Actinobacteria* and a significant increase in *Bacteroidetes* and *Clostridiales* in $Glp2r^{-/-}$ mice (Fig. 6).

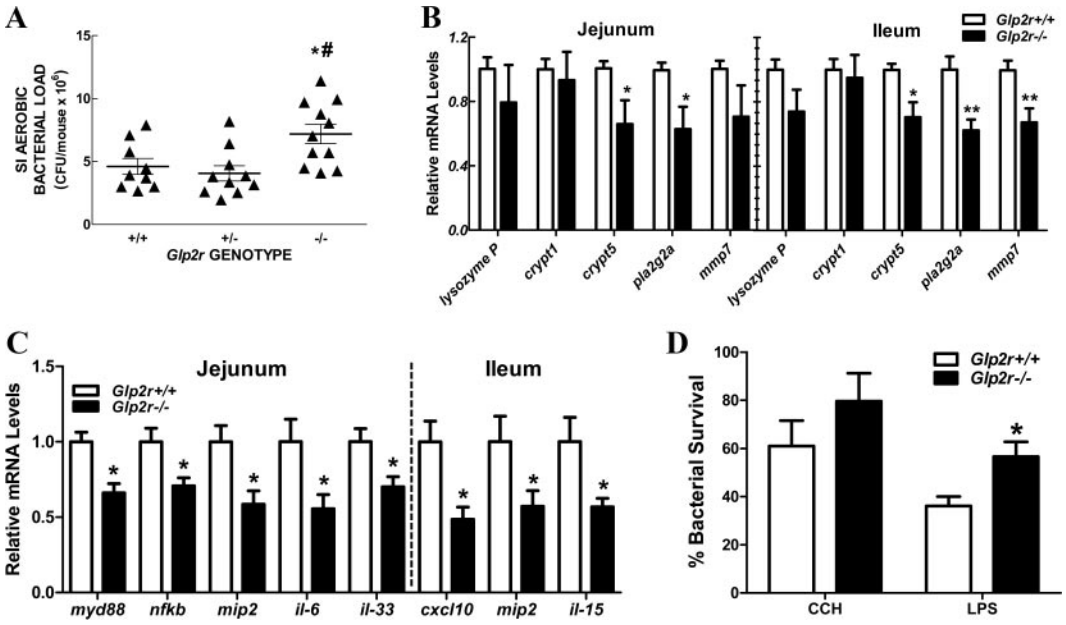

FIG. 5. Intestinal bacterial load, gene expression profiles, and intestinal bactericidal activity in $Glp2r^{-/-}$ mice. A, Small intestinal aerobic bacterial load from $Glp2r^{+/+}$, $Glp2r^{+/-}$, and $Glp2r^{-/-}$ male mice (n = 11–13 per group). Each data point corresponds to one mouse. *, $P < 0.05$, and #, $P < 0.01$ for $Glp2r^{-/-}$ *vs.* $Glp2r^{+/+}$ and $Glp2r^{+/-}$, respectively. Relative mRNA levels of Paneth cell markers (B) and inflammation-related genes (C) in jejunum and ileum of male $Glp2r^{-/-}$ mice and wild-type littermate controls (n = 7–9 per group). *, $P < 0.05$, **, $P < 0.01$ $Glp2r^{-/-}$ *vs.* $Glp2r^{+/+}$. D, Small intestinal crypts isolated from $Glp2r^{+/+}$ and $Glp2r^{-/-}$ male mice (n = 4–10 per group) were stimulated with carbamylcholine (CCH) or LPS and the supernatants assayed for bactericidal activity. *, $P < 0.05$, $Glp2r^{-/-}$ *vs.* $Glp2r^{+/+}$.

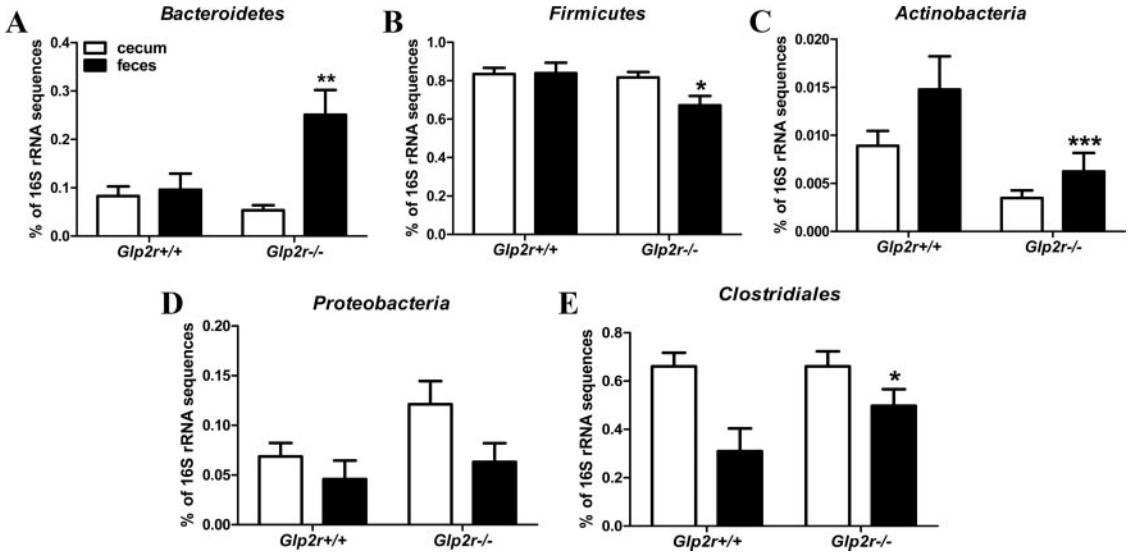

FIG. 6. 16S rRNA sequencing reveals differential expression of the gut microbiome in the feces of *Glp2r*$^{-/-}$ mice. Relative abundance of *Bacteroidetes* (A), *Firmicutes* (B), *Actinobacteria* (C), *Proteobacteria* (D), and *Clostridiales* (E) in the cecum and feces of male *Glp2r*$^{-/-}$ mice and wild-type littermates (n = 5–6 per group). *, $P < 0.05$, **, $P < 0.01$, ***, $P < 0.001$, *Glp2r*$^{-/-}$ mice *vs.* wild-type littermates.

Discussion

Current concepts of GLP-2 action have evolved primarily from studies using pharmacological administration of GLP-2R agonists, which produce expansion of the small bowel mucosal epithelium through stimulation of crypt cell proliferation and inhibition of enterocyte apoptosis (2, 33). The identification of GLP-2 (3–33) as a GLP-2R antagonist (15) has enabled experiments delineating the importance of endogenous GLP-2 action *in vivo*. These studies demonstrated that GLP-2 (3–33) attenuates the adaptive mucosal response to refeeding in mice (12) and rats (13). Nevertheless, as GLP-2 (3–33) is also a partial agonist and augments intestinal mucosal growth (15), we generated *Glp2r*$^{-/-}$ mice as an alternative model for assessing complete loss of endogenous GLP-2 action *in vivo* (8, 18, 19). Surprisingly, despite the potent intestinotrophic actions of exogenous GLP-2, crypt cell proliferation, mucosal histology, and cell lineage allocation within the gut epithelium are comparable in *Glp2r*$^{+/+}$ *vs.* *Glp2r*$^{-/-}$ mice. These findings are consistent with observations that the growth-promoting actions of GLP-2 occur predominantly at pharmacological levels of circulating GLP-2 in the parenterally fed neonatal pig (34). Nevertheless, these results do not exclude the possibility that locally produced GLP-2, acting in a paracrine manner, contributes to the control of mucosal growth.

An alternative explanation for the normal development of the *Glp2r*$^{-/-}$ gastrointestinal tract invokes the possibility of a second functional GLP-2 receptor capable of responding to endogenously produced GLP-2. Indeed, treatment of Caco-2 and T84 intestinal cell lines with GLP-2 activates growth-related signal transduction pathways and stimulates cell proliferation despite the absence of expression of the classical GLP-2R in these two cell lines (35–37). Similarly GLP-2 stimulates cell migration in multiple intestinal cell lines, despite the absence of *Glp2r* mRNA transcripts encoding the known cloned GLP-2R (38, 39). Although the existence of a second receptor responsive to exogenous GLP-2 cannot be excluded by our data, the *Glp2r*$^{-/-}$ mouse fails to up-regulate immediate early gene expression, crypt cell proliferation, or small and large bowel growth in response to exogenous GLP-2 administration. In contrast, *Glp2r*$^{-/-}$ mice exhibit a robust intestinotrophic response to exogenous IGF-I or KGF, implying preservation of growth factor-dependent pathways in both the small and large bowel. Hence, the available data suggest that the *Glp2r* gene functionally disrupted in *Glp2r*$^{-/-}$ mice encodes for the major GLP-2-responsive receptor transducing classical GLP-2 actions in the murine gastrointestinal tract.

A second explanation for the surprisingly normal phenotype of *Glp2r*$^{-/-}$ mice involves the up-regulation of related pathways compensating for the lack of GLP-2R action in the gastrointestinal tract. Our current understanding of GLP-2 action involves recruitment of downstream mediators, including IGF-I, KGF, vasoactive intestinal polypeptide , endothelial nitric oxide synthase, and ErbB ligands (16–19, 40–42). Although we have not detected evidence for up-regulation of components of the IGF-I, KGF, or ErbB pathways in the gut of the *Glp2r*$^{-/-}$ mice, our analyses have involved a limited examination of basal levels of mRNA transcripts encoding key mediators in these pathways (18, 19), and we cannot exclude the

possibility that the activity of one or more downstream targets of GLP-2 action is significantly up-regulated in a compensatory manner in *Glp2r*$^{-/-}$ mice.

Despite previous studies demonstrating proliferative and therapeutic actions of GLP-2 in the normal (16, 43, 44) and diseased (22, 30) colon, the severity of weight loss and colonic mucosal damage was comparable in the presence or absence of the *Glp2r*. Hence, GLP-2R signaling appears dispensable for the adaptive colonic response to mucosal injury in our model of DS-induced colitis. In contrast, *Glp2r*$^{-/-}$ mice exhibit greater susceptibility to indomethacin-induced enteritis, in association with increased evidence for bacterial infection in peripheral tissues, particularly mesenteric lymph nodes. Similarly, *Glp2r*$^{-/-}$ mice exhibited greater intestinal injury and more pronounced bacteremia after the administration of irinotecan, a potent topoisomerase inhibitor. Hence, the disruption of basal GLP-2R signaling appears to preferentially affect the small, rather than the large, bowel.

Consistent with findings of enhanced bacterial translocation in *Glp2r*$^{-/-}$ mice with experimental small bowel injury, levels of mRNA transcripts for the Paneth cell-derived defensin *cryptdin 5*, the antimicrobial enzyme *Pla2g2a* and associated enzymatic activators of defensin activity such as *Mmp7*, were significantly reduced in the *Glp2r*$^{-/-}$ small bowel. Furthermore, the *Glp2r*$^{-/-}$ small bowel exhibited reduced expression of multiple genes important for different components of the inflammatory response and increased bacterial content. Collectively, these observations point to one or more defects in the regulation of the epithelial-microbiota relationship in *Glp2r*$^{-/-}$ mice, findings supported by the demonstration that *Glp2r*$^{-/-}$ Paneth cell secretions exhibit reduced bactericidal activity *ex vivo*. Furthermore, significant alterations in the proportion of major bacterial microbiome constituents were detected in feces of uninjured *Glp2r*$^{-/-}$ mice. At present, we cannot ascertain whether the Paneth cell defects observed reflect loss of GLP-2 action indirectly on Paneth cells or whether these defects are secondary to other cellular phenotypes arising in *Glp2r*$^{-/-}$ mice.

Complementary evidence linking GLP-2 action to modulation of gut inflammation derives from observations that probiotic administration increased levels of GLP-2 and reduced gut inflammation in obese mice, whereas reduction of GLP-2 activity with the antagonist GLP-2 (3–33) reversed many of the beneficial antiinflammatory actions of GLP-2 (45). Similarly, GLP-2R activation suppressed intestinal leukocyte infiltration and reduced the expression of genes regulating inflammation and barrier function in a murine model of surgical ileus (46) and in mice with experimental ileitis and colitis (40). Taken together, our findings establish the importance of the intestinal *Glp2r* for the regulation of host bacterial interactions and reveal a new role for GLP-2 in Paneth cell-derived enteric defense, and control of gut microbial communities. It is important to recognize that Paneth cell activity represents only one component of an integrated intestinal and immune network that defends the mucosal epithelium from bacterial invasion. Furthermore, our data indicate that loss of the *Glp2r* clearly impairs the small bowel inflammatory response to mucosal injury. Hence, we cannot rule out other subtle abnormalities in distinct arms of the local innate immune response that contribute to the phenotypes observed in *Glp2r*$^{-/-}$ mice. Taken together, these findings establish the *Glp2r* as an essential mediator of the small bowel mucosal response to pathogens and inflammation. Whether enhancement of GLP-2 activity may be beneficial in human intestinal diseases characterized by enhanced inflammation (47) requires more careful investigation.

Acknowledgments

S.-J.L., J.L., K.K.L., D.H., H.G., D.S.G., and B.Y. carried out the experiments, analyzed the data, and wrote the manuscript. B.Y. and D.J.D. designed the experiments, and D.J.D. also wrote the manuscript. We thank Jennifer Estall for technical assistance with antisera characterization.

Address all correspondence and requests for reprints to: Daniel J. Drucker, Mt. Sinai Hospital SLRI, 600 University Avenue, TCP5-1004, Toronto, Ontario, Canada M5G 1X5. E-mail: d.drucker@utoronto.ca.

This work was supported by Canadian Institutes for Health Research Grant MOP-14799.

Disclosure Summary: None of the authors have any disclosures directly related to this manuscript. D.J.D., NPS Pharmaceuticals, the University of Toronto, and the University Health Network are parties to an agreement for licensing of GLP-2 patents.

References

1. **Brubaker PL, Crivici A, Izzo A, Ehrlich P, Tsai CH, Drucker DJ** 1997 Circulating and tissue forms of the intestinal growth factor, glucagon-like peptide-2. Endocrinology 138:4837–4843
2. **Drucker DJ, Erlich P, Asa SL, Brubaker PL** 1996 Induction of intestinal epithelial proliferation by glucagon-like peptide 2. Proc Natl Acad Sci USA 93:7911–7916
3. **Guan X, Stoll B, Lu X, Tappenden KA, Holst JJ, Hartmann B, Burrin DG** 2003 GLP-2-mediated up-regulation of intestinal blood flow and glucose uptake is nitric oxide-dependent in TPN-fed piglets 1. Gastroenterology 125:136–147
4. **Bremholm L, Hornum M, Henriksen BM, Larsen S, Holst JJ** 2009 Glucagon-like peptide-2 increases mesenteric blood flow in humans. Scand J Gastroenterol 44:314–319
5. **Benjamin MA, McKay DM, Yang PC, Cameron H, Perdue MH**

2000 Glucagon-like peptide-2 enhances intestinal epithelial barrier function of both transcellular and paracellular pathways in the mouse. Gut 47:112–119
6. **Cheeseman CI** 1997 Upregulation of SGLT-1 transport activity in rat jejunum induced by GLP-2 infusion *in vivo*. Am J Physiol 273: R1965–R1971
7. **Cottrell JJ, Stoll B, Buddington RK, Stephens JE, Cui L, Chang X, Burrin DG** 2006 Glucagon-like peptide-2 protects against TPN-induced intestinal hexose malabsorption in enterally refed piglets. Am J Physiol Gastrointest Liver Physiol 290:G293–G300
8. **Hsieh J, Longuet C, Maida A, Bahrami J, Xu E, Baker CL, Brubaker PL, Drucker DJ, Adeli K** 2009 Glucagon-like peptide-2 increases intestinal lipid absorption and chylomicron production via CD36. Gastroenterology 137:997–1005, 1005.e1–4
9. **Meier JJ, Nauck MA, Pott A, Heinze K, Goetze O, Bulut K, Schmidt WE, Gallwitz B, Holst JJ** 2006 Glucagon-like peptide 2 stimulates glucagon secretion, enhances lipid absorption, and inhibits gastric acid secretion in humans. Gastroenterology 130:44–54
10. **Jeppesen PB, Sanguinetti EL, Buchman A, Howard L, Scolapio JS, Ziegler TR, Gregory J, Tappenden KA, Holst J, Mortensen PB** 2005 Teduglutide (ALX-0600), a dipeptidyl peptidase IV resistant glucagon-like peptide 2 analogue, improves intestinal function in short bowel syndrome patients. Gut 54:1224–1231
11. **Jeppesen PB, Gilroy R, Pertkiewicz M, Allard JP, Messing B, O'Keefe SJ** 2011 Randomised placebo-controlled trial of teduglutide in reducing parenteral nutrition and/or intravenous fluid requirements in patients with short bowel syndrome. Gut 60: 902–914
12. **Shin ED, Estall JL, Izzo A, Drucker DJ, Brubaker PL** 2005 Mucosal adaptation to enteral nutrients is dependent on the physiologic actions of glucagon-like peptide-2 in mice. Gastroenterology 128: 1340–1353
13. **Nelson DW, Murali SG, Liu X, Koopmann MC, Holst JJ, Ney DM** 2008 Insulin-like growth factor I and glucagon-like peptide-2 responses to fasting followed by controlled or ad libitum refeeding in rats. Am J Physiol Regul Integr Comp Physiol 294:R1175–R1184
14. **Hartmann B, Thulesen J, Hare KJ, Kissow H, Orskov C, Poulsen SS, Holst JJ** 2002 Immunoneutralization of endogenous glucagon-like peptide-2 reduces adaptive intestinal growth in diabetic rats. Regul Pept 105:173–179
15. **Thulesen J, Knudsen LB, Hartmann B, Hastrup S, Kissow H, Jeppesen PB, Ørskov C, Holst JJ, Poulsen SS** 2002 The truncated metabolite GLP-2 (3–33) interacts with the GLP-2 receptor as a partial agonist. Regul Pept 103:9–15
16. **Ørskov C, Hartmann B, Poulsen SS, Thulesen J, Hare KJ, Holst JJ** 2005 GLP-2 stimulates colonic growth via KGF, released by subepithelial myofibroblasts with GLP-2 receptors. Regul Pept 124: 105–112
17. **Dubé PE, Forse CL, Bahrami J, Brubaker PL** 2006 The essential role of insulin-like growth factor-1 in the intestinal tropic effects of glucagon-like peptide-2 in mice. Gastroenterology 131:589–605
18. **Yusta B, Holland D, Koehler JA, Maziarz M, Estall JL, Higgins R, Drucker DJ** 2009 ErbB signaling is required for the proliferative actions of GLP-2 in the murine gut. Gastroenterology 137: 986–996
19. **Bahrami J, Yusta B, Drucker DJ** 2010 ErbB activity links the glucagon-like peptide-2 receptor to refeeding-induced adaptation in the murine small bowel. Gastroenterology 138:2447–2456
20. **Bahrami J, Longuet C, Baggio LL, Li K, Drucker DJ** 2010 The glucagon-like peptide-2 receptor modulates islet adaptation to metabolic stress in the ob/ob mouse. Gastroenterology 139:857–868
21. **Boushey RP, Yusta B, Drucker DJ** 1999 Glucagon-like peptide 2 decreases mortality and reduces the severity of indomethacin-induced murine enteritis. Am J Physiol 277:E937–E947
22. **Drucker DJ, Yusta B, Boushey RP, DeForest L, Brubaker PL** 1999 Human [Gly2]-GLP-2 reduces the severity of colonic injury in a murine model of experimental colitis. Am J Physiol 276:G79–G91
23. **Boushey RP, Yusta B, Drucker DJ** 2001 Glucagon-like peptide (GLP)-2 reduces chemotherapy-associated mortality and enhances cell survival in cells expressing a transfected GLP-2 receptor. Cancer Res 61:687–693
24. **Hedo JA, Kahn CR** 1985 Radioactive labeling and turnover studies of the insulin receptor subunits. Methods Enzymol 109:593–609
25. **Koehler JA, Yusta B, Drucker DJ** 2005 The HeLa cell glucagon-like peptide-2 receptor is coupled to regulation of apoptosis and ERK1/2 activation through divergent signaling pathways. Mol Endocrinol 19:459–473
26. **Bjerknes M, Cheng H** 1981 Methods for the isolation of intact epithelium from the mouse intestine. Anat Rec 199:565–574
27. **Ayabe T, Satchell DP, Wilson CL, Parks WC, Selsted ME, Ouellette AJ** 2000 Secretion of microbicidal alpha-defensins by intestinal Paneth cells in response to bacteria. Nat Immunol 1:113–118
28. **Ley RE, Bäckhed F, Turnbaugh P, Lozupone CA, Knight RD, Gordon JI** 2005 Obesity alters gut microbial ecology. Proc Natl Acad Sci USA 102:11070–11075
29. **Wang Q, Garrity GM, Tiedje JM, Cole JR** 2007 Naive Bayesian classifier for rapid assignment of rRNA sequences into the new bacterial taxonomy. Appl Environ Microbiol 73:5261–5267
30. **L'Heureux MC, Brubaker PL** 2003 Glucagon-like peptide-2 and common therapeutics in a murine model of ulcerative colitis. J Pharmacol Exp Ther 306:347–354
31. **Munroe DG, Gupta AK, Kooshesh F, Vyas TB, Rizkalla G, Wang H, Demchyshyn L, Yang ZJ, Kamboj RK, Chen H, McCallum K, Sumner-Smith M, Drucker DJ, Crivici A** 1999 Prototypic G protein-coupled receptor for the intestinotrophic factor glucagon-like peptide 2. Proc Natl Acad Sci USA 96:1569–1573
32. **Yusta B, Huang L, Munroe D, Wolff G, Fantaske R, Sharma S, Demchyshyn L, Asa SL, Drucker DJ** 2000 Enteroendocrine localization of GLP-2 receptor expression. Gastroenterology 119:744–755
33. **Tsai CH, Hill M, Asa SL, Brubaker PL, Drucker DJ** 1997 Intestinal growth-promoting properties of glucagon-like peptide 2 in mice. Am J Physiol 273:E77–E84
34. **Burrin DG, Stoll B, Guan X, Cui L, Chang X, Holst JJ** 2005 Glucagon-like peptide 2 dose-dependently activates intestinal cell survival and proliferation in neonatal piglets. Endocrinology 146: 22–32
35. **Jasleen J, Shimoda N, Shen ER, Tavakkolizadeh A, Whang EE, Jacobs DO, Zinner MJ, Ashley SW** 2000 Signaling mechanisms of glucagon-like peptide 2-induced intestinal epithelial cell proliferation. J Surg Res 90:13–18
36. **Jasleen J, Ashley SW, Shimoda N, Zinner MJ, Whang EE** 2002 Glucagon-like peptide 2 stimulates intestinal epithelial proliferation in vitro. Dig Dis Sci 47:1135–1140
37. **Rocha FG, Shen KR, Jasleen J, Tavakkolizadeh A, Zinner MJ, Whang EE, Ashley SW** 2004 Glucagon-like peptide-2: divergent signaling pathways. J Surg Res 121:5–12
38. **Bulut K, Meier JJ, Ansorge N, Felderbauer P, Schmitz F, Hoffmann P, Schmidt WE, Gallwitz B** 2004 Glucagon-like peptide 2 improves intestinal wound healing through induction of epithelial cell migration *in vitro* evidence for a TGF-β-mediated effect. Regul Pept 121: 137–143
39. **Masur K, Schwartz F, Entschladen F, Niggemann B, Zaenker KS** 2006 DPPIV inhibitors extend GLP-2 mediated tumour promoting effects on intestinal cancer cells. Regul Pept 137:147–155
40. **Sigalet DL, Wallace LE, Holst JJ, Martin GR, Kaji T, Tanaka H, Sharkey KA** 2007 Enteric neural pathways mediate the anti-inflammatory actions of glucagon-like peptide 2. Am J Physiol Gastrointest Liver Physiol 293:G211–G221
41. **Amato A, Baldassano S, Serio R, Mulè F** 2009 Glucagon-like peptide-2 relaxes mouse stomach through vasoactive intestinal peptide release. Am J Physiol Gastrointest Liver Physiol 296: G678–G684
42. **Guan X, Karpen HE, Stephens J, Bukowski JT, Niu S, Zhang G, Stoll**

B, Finegold MJ, Holst JJ, Hadsell D, Hadsell DL, Nichols BL, Burrin DG 2006 GLP-2 receptor localizes to enteric neurons and endocrine cells expressing vasoactive peptides and mediates increased blood flow. Gastroenterology 130:150–164

43. **Litvak DA, Hellmich MR, Evers BM, Banker NA, Townsend Jr CM** 1998 Glucagon-like peptide 2 is a potent growth factor for small intestine and colon. J Gastrointest Surg 2:146–150
44. **Ghatei MA, Goodlad RA, Taheri S, Mandir N, Brynes AE, Jordinson M, Bloom SR** 2001 Proglucagon-derived peptides in intestinal epithelial proliferation: glucagon-like peptide-2 is a major mediator of intestinal epithelial proliferation in rats. Dig Dis Sci 46:1255–1263
45. **Cani PD, Possemiers S, Van de Wiele T, Guiot Y, Everard A, Rottier O, Geurts L, Naslain D, Neyrinck A, Lambert DM, Muccioli GG, Delzenne NM** 2009 Changes in gut microbiota control inflammation in obese mice through a mechanism involving GLP-2-driven improvement of gut permeability. Gut 58:1091–1103
46. **Moore BA, Peffer N, Pirone A, Bassiri A, Sague S, Palmer JM, Johnson DL, Nesspor T, Kliwinski C, Hornby PJ** 2010 GLP-2 receptor agonism ameliorates inflammation and gastrointestinal stasis in murine postoperative ileus. J Pharmacol Exp Ther 333:574–583
47. **Buchman AL, Katz S, Fang JC, Bernstein CN, Abou-Assi SG** 2010 Teduglutide, a novel mucosally active analog of glucagon-like peptide-2 (GLP-2) for the treatment of moderate to severe Crohn's disease. Inflamm Bowel Dis 16:962–973